European Journal of Chemistry 5 (1) (2014) 53-64

European Journal of Chemistry

Journal homepage: www.eurjchem.com

Influence of some synthesized pyrimidine derivatives on corrosion inhibition of mild steel in hydrochloric acid medium

Doddahosuru Mahadevappa Gurudatt and Kikkeri Narasimha Shetty Mohana *

Department of Studies in Chemistry, University of Mysore, Manasagangothri, Mysore 570 006, India

**Corresponding author at: Department of Studies in Chemistry, University of Mysore, Manasagangothri, Mysore 570 006, India. Tel.: +91.821.2419654. Fax: +91.821.2421263. E-mail address: drknmohana@gmail.com (K.N. Mohana).*

ARTICLE INFORMATION

DOI: 10.5155/eurjchem.5.1.53-64.899

Received: 27 July 2013
Received in revised form: 30 August 2013
Accepted: 30 August 2013
Online: 31 March 2014

KEYWORDS

Inhibition
Mild steel
Weight loss
Polarization
Scanning electron microscopy
Electrochemical impedance spectroscopy

ABSTRACT

The influence of four newly synthesized pyrimidine derivatives on the corrosion inhibition of mild steel in 0.5 M HCl solution is studied using mass loss and electrochemical techniques. The corrosion rate was found to depend on concentration and temperature of the medium. Adsorption of all the four inhibitors obeys Langmuir isotherm model. Polarization curves indicated that the studied inhibitors are of mixed type. Electrochemical impedance spectroscopy explains the mechanism of inhibitor's action. Various activation and adsorption thermodynamic parameters were calculated and discussed. The results obtained from weight loss and electrochemical studies are in good agreement with each other. The variation in inhibitive efficiency mainly depends on the type and nature of the substituents present in the inhibitor molecule.

1. Introduction

The corrosion of iron and mild steel is a fundamental academic and industrial concern that has received a considerable amount of attention [1]. Aqueous solution of acids is among the most corrosive media. Hydrochloric acid solutions are widely used in several industrial processes such as acid pickling, acid cleaning, acid de-scaling and oil well acidizing [2]. Corrosion inhibitors are of great practical importance, being extensively employed in minimising metallic waste in engineering materials [3]. Most efficient inhibitors are organic compounds containing electronegative functional groups and π-electrons in triple or conjugated double bonds. The remarkable inhibitory effect is reinforced by the presence of heteroatom such as sulphur, nitrogen and oxygen in the ring which facilitates its adsorption on the metal surface following the sequence O < N < S [4].

The adsorption on the metal surface depends mainly on the physicochemical properties of the inhibitor group such as the functional group, molecular electronic structure, electronic density at the donor atom, *p*-orbital character and the molecular size [5]. These inhibitors have extended *p*-electron systems and functional groups such as -C=C-, -OR, -OH, -NR and –SR. The functional groups provide electrons that facilitate the adsorption of the inhibitor on the metal surface [6]. *N*-Heterocyclic compounds are well qualified to play more protection for steel corrosion [7]. Many *N*-heterocyclic compounds such as derivatives of pyrazole [8], triazole [9], tetrazole [10], imidazole [11], pyridine [12], pyrimidine [13-15], and pyridazine [16] has been reported as effective corrosion inhibitors for mild steel in acidic media. The heterocyclic compounds containing nitrogen atoms can easily be protonated in acidic medium to exhibit good inhibitory action on the corrosion of metals in acid solutions. Hackermann and Makrides pointed out that sulphur containing organic compounds have better inhibitive efficiency due to better electron donor capacity and easy polarisability. Due to the above reasons, sulphur containing organic compounds has been recognized as better inhibitors [17]. Ayre *et al*. showed that substances containing atoms of both nitrogen and sulphur containing heterocyclic compounds are found to be excellent inhibitors in HCl solutions [18]. The selection of pyrimidine derivatives as corrosion inhibitor based on the presence of sulfur and nitrogen atoms, which could possibly serve as active sites for the adsorption process.

The present study aimed to synthesize the pyrimidine derivatives as corrosion inhibitors for mild steel in 0.5 M hydrochloric acidic medium. The experimental findings were discussed with various activation and adsorption thermodynamic parameters. The protective film formed on the metal surface was characterized by SEM. Finally, evaluation of inhibitor efficiency was discussed.

ISSN 2153-2249 (Print) / ISSN 2153-2257 (Online)
http://dx.doi.org/10.5155/eurjchem.5.1.53-64.899

Table 1. The abbreviations, molecular structures and names of pyrimidine derivatives.

Abbreviation	Molecular structure	Name
P1	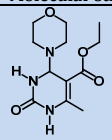	6-Methyl-4-morpholin-4-yl-2-oxo-1,2,3,4-tetrahydro-pyrimidine-5-carboxylic acid ethyl ester
P2	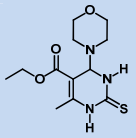	6-Methyl-4-morpholin-4-yl-2-thioxo-1,2,3,4-tetrahydro-pyrimidine-5-carboxylic acid ethyl ester
P3	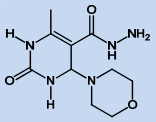	6-Methyl-4-morpholin-4-yl-2-oxo-1,2,3,4-tetrahydro-pyrimidine-5-carboxylic acid hydrazide
P4	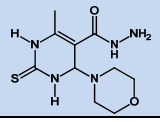	6-Methyl-4-morpholin-4-yl-2-thioxo-1,2,3,4-tetrahydro-pyrimidine-5-carboxylic acid hydrazide

2. Experimental

2.1. Materials and sample preparation

Mild steel (MS) specimens used in the present study having the chemical compositions (in wt %) of C - 0.051; Mn - 0.179; Si - 0.006; P - 0.005; S - 0.023; Cr - 0.051; Ni - 0.05; Mo - 0.013; Ti - 0.004; Al - 0.103; Cu - 0.050; Sn - 0.004; B - 0.00105; Co - 0.017; Nb - 0.012; Pb - 0.001 and the remainder iron. Prior to gravimetric and electrochemical measurements, the surface of the specimens was polished under running tap water using SiC emery paper up to 1200 grade, rinsed with distilled water, dried on a clean tissue paper, immersed in benzene for 5 sec, dried and then immersed in acetone for 5 sec and dried with clean tissue paper. Finally, the specimens were kept in desiccators until use. At the end of the test, the specimens were carefully washed with benzene and acetone, dried and then weighed. Appropriate concentrations of acid were prepared by using double-distilled water. The concentration range of inhibitor employed was 0.05 g/L to 0.25 g/L.

2.2. Synthesis of inhibitors

The synthesis of pyrimidine derivatives is outlined in Scheme 1. In a typical experimental procedure a solution of β-ketoester, aldehyde and urea/thiourea in ethanol was heated reflux in the presence of catalytic amount of $CaCl_2$ to give 6-methyl-4-morpholin-4-yl-2-(oxo/thioxo)-1,2,3,4-tetrahydro-pyrimidine-5-carboxylic acid ethyl ester (P1/P2) followed by reaction with hydrazine hydrate in ethanol to give 6-methyl-4-morpholin-4-yl-2-(oxo/thioxo)-1,2,3,4-tetrahydro-pyrimidine-5-carboxylic acid hydrazide (P3/P4) [19]. The structure of all the synthesized compounds was established by IR, ^{1}H NMR and Mass spectral analyses. The abbreviations, molecular structures and names of all the four pyrimidine derivatives are given in Table 1.

All the solvents and chemicals used were of analytical reagent grade and used as such. FTIR spectra were recorded using a Jasco FTIR 4100 double beam spectrometer. ^{1}H-NMR spectra were recorded on Bruker DRX-500 spectrometer at 400 MHz using DMSO-d_6 as solvent and TMS as an internal standard. LC Mass spectra were recorded using Agilent-SC/AD/10-017 instrument.

6-Methyl-4-morpholin-4-yl-2-oxo-1,2,3,4-tetrahydro-pyrimidine-5-carboxylic acid ethyl ester (**P1**): IR (KBr, ν cm^{-1}): 3350, 2225, (NH), 1726.2 (C=O ester), 1708.8 (C=O, ketonic), 1700 (-C-O-), 1652 (O-C_2H_5), 1600.8 (C=C), 1261 (C–N), 1120 (C-O-C). ^{1}H NMR (400 MHz, DMSO-d_6, δ, ppm): 1.30 (q, *J* = 6.6 Hz, 2H, ester CH_2), 1.71 (s, 3H, CH_3), 2.37 (m, 4H, CH_2-O-CH_2 morpholine), 3.67 (m, 4H, CH_2 -N-CH_2 morpholine), 4.19 (t, *J* = 7.2 Hz, 3H, ester CH_3), 5.41 (s, 1H, methine), 7.68 (s, 1H, N-H), 9.12 (s, 1H, N-H). MS (EI, *m/z* (%)): 269.14 (M$^+$, 100).

6-Methyl-4-morpholin-4-yl-2-thioxo-1,2,3,4-tetrahydro-pyrimidine-5-carboxylic acid ethyl ester (**P2**): IR (KBr, ν cm^{-1}): 3345, 2234 (NH), 1735 (C=O), 1705 (-C-O-), 1703.0 (C=C), 1658 (O-C_2H_5), 1304 (C–N), 1270-1190 (-C=S). ^{1}H NMR (400 MHz, DMSO-d_6, δ, ppm): 1.28 (q, 2H, ester CH_2 6.6), 1.82 (s, 3H, CH_3), 2.39 (m, 4H, CH_2-O-CH_2 morpholine), 3.71 (m, 4H, CH_2 -N-CH_2 morpholine), 4.24 (t, *J* = 6.9 Hz, 3H, ester CH_3), 5.53 (s, 1H, methine), 7.73 (s, 1H, N-H), 8.93 (s, 1H, N-H). MS (EI, *m/z* (%)):285.14 (M$^+$, 100).

6-Methyl-4-morpholin-4-yl-2-oxo-1,2,3,4-tetrahydro-pyrimidine-5-carboxylic acid hydrazide (**P3**): IR (KBr, ν cm^{-1}): 3442, 3425, 1689 (hydrazide), 3355, 2238, (NH), 1712(C=O ketonic), 1610 (C=C), 1332 (C–N), 1123 (C-O-C). ^{1}H NMR (400 MHz, DMSO-d_6, δ, ppm): 1.82 (s, 3H, CH_3), 2.34 (m, 4H, CH_2-O-CH_2 morpholine), 2.60 (s, 2H, hydrazide NH_2), 3.62 (m, 4H, CH_2 -N-CH_2 morpholine), 5.57 (s, 1H, methine), 7.73 (s, 1H, N-H), 8.30 (s, 1H, hydrazide NH), 8.93 (s, 1H, N-H). MS (EI, *m/z* (%)):255.11 (M$^+$, 100).

6-Methyl-4-morpholin-4-yl-2-thioxo-1,2,3,4-tetrahydro-pyrimidine-5-carboxylic acid hydrazide (**P4**): IR (KBr, ν cm^{-1}): 3448, 3415, 1675 (hydrazide), 3350, 2242 (NH), 1304 (C–N), 1270-1190 (-C=S), 1120 (C–O–C). ^{1}H NMR (400 MHz, DMSO-d_6, δ, ppm): 1.90 (s, 3H, CH_3), 2.39 (m, 4H, CH_2-O-CH_2 morpholine), 2.9 (s, 2H, (hydrazide NH_2), 3.67 (m, 4H, CH_2-N-CH_2 morpholine), 5.48 (s, 1H, methine), 7.65 (s, 1H, N-H), 8.70 (s, 1H, hydrazide NH), 8.87 (s, 1H, N-H). MS (EI, *m/z* (%)):271.11 (M$^+$, 100).

2.3. Weight loss measurements

Mild steel specimens were immersed in the acid solutions for 6 h at different temperature. The temperature of the environment was maintained by thermostatically controlled water bath with accuracy of ±0.2 °C (Weiber Limited, Chennai, India), under aerated condition.

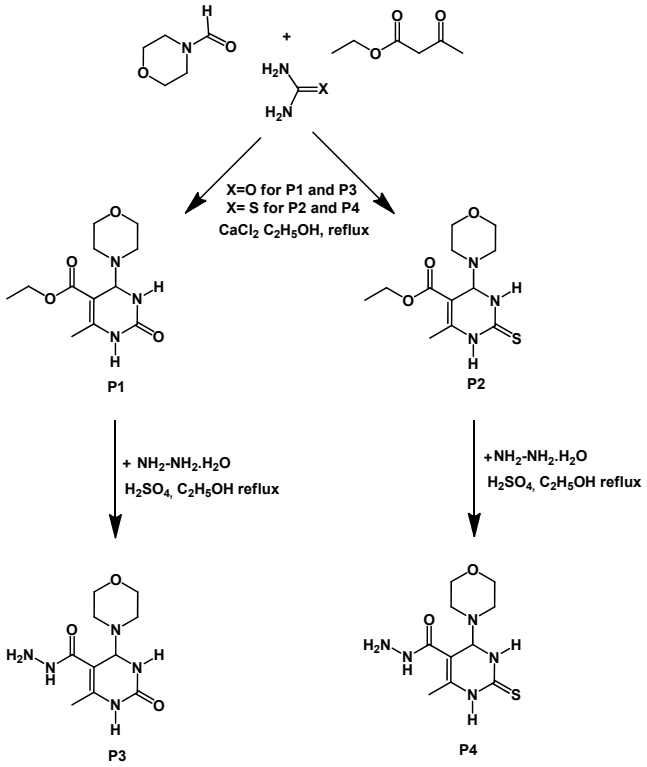

Scheme 1

After 6 h of immersion the specimens were removed, rinsed in water and acetone, and dried in desiccators. The weight loss was recorded to the nearest 0.0001 gram by using an analytical balance (Sartorius, precision ±0.1 mg). The average weight loss of three parallel specimens was obtained. Relative weight losses of the specimens were used to calculate the percent inhibition efficiency (η %). Then the tests were repeated with different concentrations of the inhibitor at varying temperatures.

2.4. Electrochemical measurements

Polarization and Electrochemical Impedance Spectroscopy (EIS) experiments were carried out using a CHI660D electrochemical workstation. A conventional three-electrode cell consisting of a saturated calomel reference electrode (SCE), a platinum auxiliary electrode and the working electrode with 1 cm^2 exposed area of MS specimen was used. The specimens were pre-treated similarly as done in the gravimetric measurements. The electrochemical tests were performed using the synthesized pyrimidine derivatives with various concentrations ranging from 0.05 g/L to 0.25 g/L at 30 °C. Potentiodynamic polarization measurements were performed in the potential range from -850 to -150 mV with a scan rate of 0.4 mV/s. EIS measurements were carried out at the open circuit potential (OCP). Prior to the EIS measurement, a steady-state period of 30 min was observed, which proved sufficient for OCP to attain a stable value. The ac frequency range extended from 10 kHz to 0.05 kHz with signal amplitude of ±10 mV.

2.5. Scanning Electron Microscopy (SEM)

The SEM analysis was performed using a JSM-5800 electron microscope with the working voltage of 20 kV and the working distance 24 mm. In SEM micrographs, the specimens were exposed to 0.5 M HCl in the absence and presence of inhibitors under optimum conditions after a desired period of immersion. The SEM images were taken for polished mild steel specimen and specimen immersed in solution without and with inhibitors.

3. Results and discussion

3.1. Weight loss measurements

3.1.1. Effect of inhibitor concentration

The weight loss measurements were carried out as a function of temperature (30-60 °C) and concentration (0.05 g/L to 0.25 g/L) at 6 h of immersion time. The corrosion rate (C_R) was calculated from the Equation (1).

$$C_R = \frac{\Delta W}{St} \quad (1)$$

where, ΔW is the weight loss (mg cm^{-2} h^{-1}), S is the surface area of the specimen (cm^2) and t is the immersion time (h). The corrosion inhibition efficiency η (%) was calculated according to the Equation (2).

$$\eta(\%) = \frac{(C_R)_a - (C_R)_p}{(C_R)_a} \times 100 \quad (2)$$

where $(C_R)_a$ and $(C_R)_p$ are corrosion rates in the absence and presence of the inhibitor, respectively. Weight loss data of mild steel in 0.5 M HCl in the absence and presence of various concentrations of inhibitors are tabulated in Table 2. The corrosion rate of mild steel is decreases with increase in inhibitors concentration. The inhibitor was found to attain the maximum inhibition efficiency at 0.25 g/L for all the studied inhibitors (Table 2).

Table 2. Weight loss data of mild steel corrosion in 0.5 M HCl in presence of different concentrations of the inhibitors at different temperature

Inhibitor	C *	30 °C	θ	η *	40 °C	θ	η *	50 °C	θ	η *	60 °C	θ	η *
		C_R			C_R			C_R			C_R		
Blank	0.00	0.452	-	-	0.765	-	-	0.796	-	-	1.260	-	-
P1	0.05	0.139	0.693	69.2	0.233	0.695	69.5	0.242	0.696	69.6	0.379	0.699	69.9
	0.10	0.108	0.761	76.1	0.181	0.763	76.3	0.171	0.785	78.5	0.271	0.785	78.5
	0.15	0.103	0.772	77.2	0.156	0.796	79.6	0.146	0.817	81.6	0.229	0.818	81.8
	0.20	0.092	0.796	79.6	0.144	0.812	81.2	0.122	0.847	84.7	0.188	0.851	85.1
	0.25	0.088	0.805	80.5	0.119	0.844	84.4	0.112	0.859	85.9	0.171	0.864	86.4
P2	0.05	0.138	0.695	69.5	0.223	0.709	70.8	0.232	0.709	70.8	0.354	0.719	71.9
	0.10	0.109	0.759	75.9	0.161	0.790	78.9	0.161	0.798	79.8	0.259	0.794	79.4
	0.15	0.093	0.794	79.4	0.146	0.809	80.9	0.136	0.829	82.9	0.219	0.826	82.6
	0.20	0.082	0.819	81.9	0.134	0.825	82.5	0.112	0.859	85.9	0.178	0.859	85.9
	0.25	0.078	0.827	82.7	0.117	0.847	84.7	0.086	0.892	89.2	0.126	0.900	89.9
P3	0.05	0.127	0.719	71.9	0.212	0.723	72.3	0.212	0.734	73.4	0.334	0.735	73.5
	0.10	0.099	0.781	78.1	0.151	0.803	80.3	0.151	0.810	81.0	0.239	0.810	81.0
	0.15	0.083	0.816	81.6	0.136	0.822	82.2	0.126	0.842	84.2	0.200	0.841	84.1
	0.20	0.072	0.841	84.0	0.114	0.851	85.1	0.102	0.872	87.2	0.161	0.872	87.2
	0.25	0.061	0.865	86.5	0.086	0.888	88.7	0.071	0.911	91.1	0.101	0.920	91.9
P4	0.05	0.112	0.752	75.2	0.202	0.736	73.6	0.202	0.746	74.6	0.324	0.743	74.3
	0.10	0.089	0.803	80.3	0.141	0.816	81.6	0.141	0.823	82.3	0.229	0.818	81.8
	0.15	0.073	0.839	83.8	0.126	0.835	83.5	0.116	0.854	85.4	0.199	0.842	84.2
	0.20	0.062	0.863	86.3	0.104	0.864	86.4	0.092	0.884	88.4	0.151	0.880	88.0
	0.25	0.048	0.894	89.4	0.071	0.907	90.7	0.066	0.917	91.7	0.095	0.925	92.4

* C: g/L; C_R: mg.cm^{-2} h^{-1}; η: %.

This is due to the fact that, adsorption and the degree of surface coverage of inhibitor on the mild steel increases with the inhibitor concentration, thus the mild steel surface gets efficiently separated from the medium [20]. The protective property of these compounds is probably due to the interaction between p electrons and hetero atoms with positively charged steel surface [21].

3.1.2. Effect of temperature

The effect of temperature on the inhibitive performance of the synthesized pyrimidine derivatives on mild steel in 0.5 M HCl were studied in the temperature range of 30-60 °C in the absence and presence of different concentrations of inhibitor during 6 h of immersion time. It is observed that the inhibition efficiency increases with temperature (Table 2).

However, at 50 and 60 °C, it is found that a slight increase or constancy in inhibition efficiency with the increase of temperature at different concentration. This may be due to the chemical adsorption alone or due to the combination of physical and chemical adsorption (comprehensive adsorption) [22], however, beyond 60 °C inhibition efficiency decreases.

The effect of temperature on the inhibited acid-metal reaction is highly complex, because many changes occur on the metal surface such as rapid etching and desorption of inhibitor and the inhibitor itself may undergo decomposition and/or rearrangement [23].

Thermodynamic parameters such as the activation energy E_a*, the entropy of activation ΔS_a* and the enthalpy of activation ΔH_a^* for the corrosion of mild steel in the absence and presence of different concentrations of P1, P2, P3 and P4 were calculated using the following Arrhenius-type equation (3).

$$C_R = k\ exp\left(-\frac{E_a^*}{RT}\right) \quad (3)$$

An alternative formulation of the Arrhenius equation is,

$$C_R = \frac{RT}{Nh} exp\frac{\Delta S_a^*}{R} exp\left(-\frac{\Delta H_a^*}{RT}\right) \quad (4)$$

where, k is Arrhenius pre-exponential factor, h is Planck's constant, N is Avogadro's number, T is the absolute temperature and R is the universal gas constant. Using Equation (3), and from a plot of the ln C_R *versus* $1/T$ (Figure 1a-1d), the values of E_a* and k at various concentrations of P1, P2, P3 and P4 were computed from slopes and intercepts, respectively. Further, using Equation (4), plots of ln (C_R/T) *versus* $1/T$ gave straight lines (Figure 2a-2d) with a slope of (-$\Delta H_a^*/2.303R$) and an intercept of [log (R/Nh) + $\Delta S_a^*/2.303R$], from which the values of ΔH_a* and ΔS_a* were calculated and are listed in Table 3. Thermodynamic activation functions (E_a^*) of the corrosion in mild steel in 0.5 M HCl in the presence of the inhibitors are lower than those in the uninhibited solution, indicating that all the inhibitors exhibit high inhibition efficiency at elevated temperatures [24].

The positive sign of the enthalpy (ΔH_a*) reflects the endothermic nature of the mild steel dissolution process [25,26]. The negative values of ΔS_a* for all four inhibitors indicates that the formation of the activated complex in the rate-determining step represents an association rather than a dissociation step, meaning that a decrease in disorder takes place during the course of the transition from reactants to activated complex [27].

3.1.3. Adsorption isotherm

The dependence of the degree of surface coverage (θ) as function of concentration (C) of the inhibitor was tested graphically by fitting it to various isotherms to find the best isotherm which describes this study. Langmuir adsorption isotherm was found to be the best description for all four synthesized pyrimidine derivatives on mild steel. According to this isotherm, θ is related to the inhibitor concentration, C and adsorption equilibrium constant K_{ads}, as

$$\frac{C}{\theta} = \frac{1}{K_{ads}} + C \quad (5)$$

The plot of C/θ versus C gave a straight line (Figure 3a-3d) with a slope of around unity confirming that the adsorption of pyrimidine derivatives on mild steel surface in 0.5 M HCl obeys the Langmuir adsorption isotherm. According to Langmuir adsorption isotherm there is no interaction between the adsorbed inhibitor molecules, and the energy of adsorption is independent on the degree of surface coverage (θ).

Langmuir isotherm assumes that the solid surface contains a fixed number of adsorption sites and each site occupies one adsorbed species.

The equilibrium adsorption constant, K_{ads} is related to the standard Gibb's free energy of adsorption (ΔG_{ads}) with the following equation:

$$K_{ads} = \frac{1}{55.5} exp\left[\frac{\Delta G_{ads}}{RT}\right] \quad (6)$$

Table 3. Activation parameters for mild steel in 0.5 M HCl in the absence and presence of different concentrations of P1, P2, P3 and P4.

Inhibitor	C (g/L)	E_a* (kJ/mol)	ΔH_a* (kJ/mol)	ΔS_a* (J/mol.K)
P1	0.00	26.15	24.53	-170.25
	0.05	25.58	22.95	-185.28
	0.10	10.77	20.05	-196.85
	0.15	19.52	16.89	-207.92
	0.20	16.59	13.49	-220.64
	0.25	16.13	13.96	-218.32
P2	0.00	26.15	24.53	-170.25
	0.05	24.05	21.42	-190.43
	0.10	21.72	19.08	-194.74
	0.15	20.93	18.30	-191.02
	0.20	18.01	15.38	-214.55
	0.25	9.49	06.85	-243.02
P3	0.00	26.15	24.53	-170.25
	0.05	24.35	21.72	-190.08
	0.10	22.15	19.51	-199.64
	0.15	21.50	18.86	-202.96
	0.20	19.31	16.67	-211.46
	0.25	11.07	08.43	-240.050
P4	0.00	26.15	24.53	-170.25
	0.05	26.78	24.14	-182.97
	0.10	23.76	21.12	-195.17
	0.15	24.53	21.90	-194.07
	0.20	21.38	18.73	-205.81
	0.25	16.57	13.93	-223.90

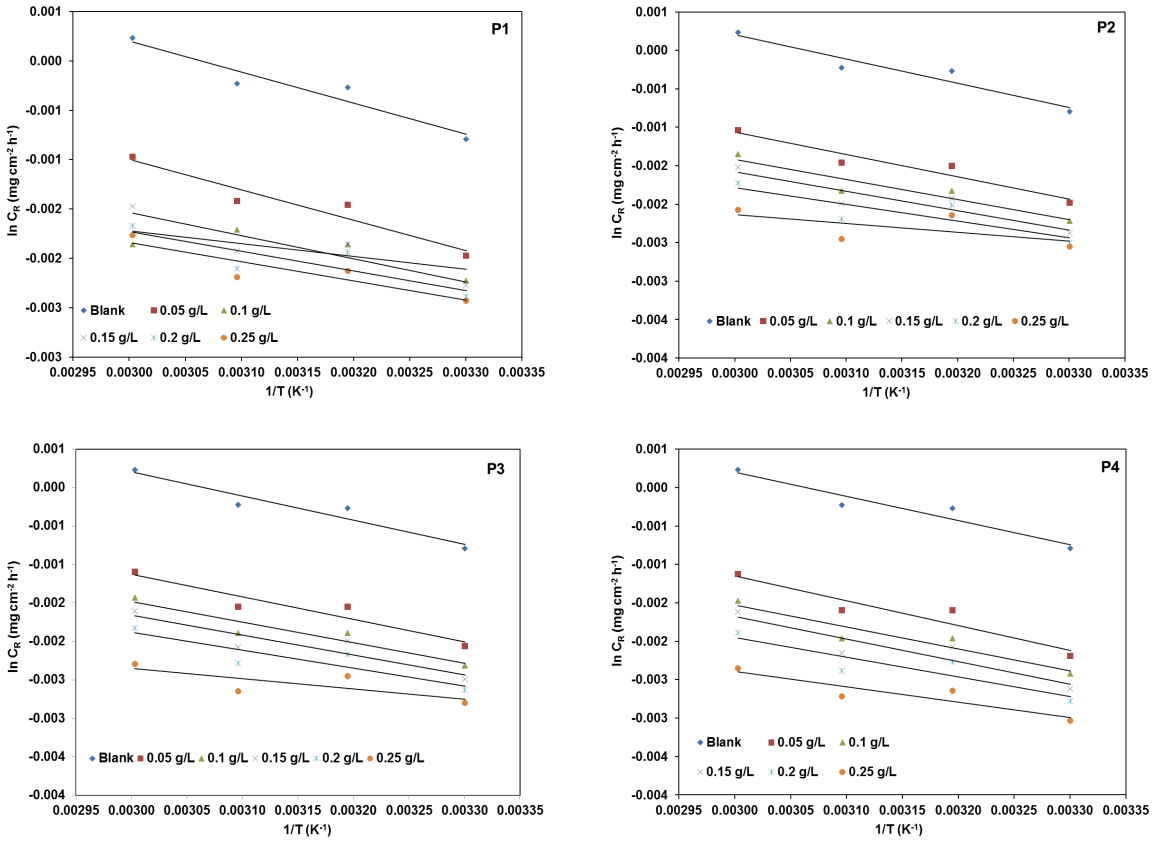

Figure 1. Arrhenius plots for the corrosion of mild steel in 0.5 M HCl in the absence and presence of different concentrations of (a) P1 (b) P2 (c) P3 and (d) P4.

where 55.5 is the concentration of water in solution (mol/L), R is the universal gas constant and T is the absolute temperature. The calculated ΔG_{ads} values of the studied pyrimidines are tabulated in Table 4. The enthalpy and entropy of adsorption (ΔH_{ads} and ΔS_{ads}) can be calculated using the Equation (7).

$$ln\ K_{ads} = ln\frac{1}{55.5} - \frac{\Delta H_{ads}}{RT} + \frac{\Delta S_{ads}}{R} \quad (7)$$

The entropy of adsorption can be calculated based on the following thermodynamic equation.

$$\Delta G_{ads} = \Delta H_{ads} - T\,\Delta S_{ads} \quad (8)$$

The negative values of ΔG_{ads} suggest that the adsorption of inhibitor molecules onto the steel surface is a spontaneous phenomenon.

Table 4. Thermodynamic parameters for adsorption of P1, P2, P3 and P4 on mild steel in 0.5 M HCl at different temperatures from Langmuir adsorption isotherm

Inhibitor	T (K)	r^2	K_{ads} (L/mol)	ΔG_{ads} (kJ/mol)	ΔH_{ads} (kJ/mol)	ΔS_{ads} (J/mol K)
P1	303	0.999	76923.08	-21.06	-42	-8.086
	313	0.999	58823.53	-21.05		
	323	0.999	58823.53	-21.73		
	333	0.999	55555.56	-22.24		
P2	303	0.999	66666.67	-20.70	-36	-9.875
	313	0.999	71428.57	-21.56		
	323	0.999	52631.58	-21.43		
	333	0.997	50000.00	-21.95		
P3	303	0.999	58823.53	-20.38	-50	-5.055
	313	0.998	58823.53	-21.05		
	323	0.998	52631.58	-21.43		
	333	0.997	50000.00	-21.95		
P4	303	0.998	62500.00	-20.53	-54	-3.845
	313	0.997	55555.56	-20.91		
	323	0.998	58823.53	-21.73		
	333	0.997	52631.58	-22.09		

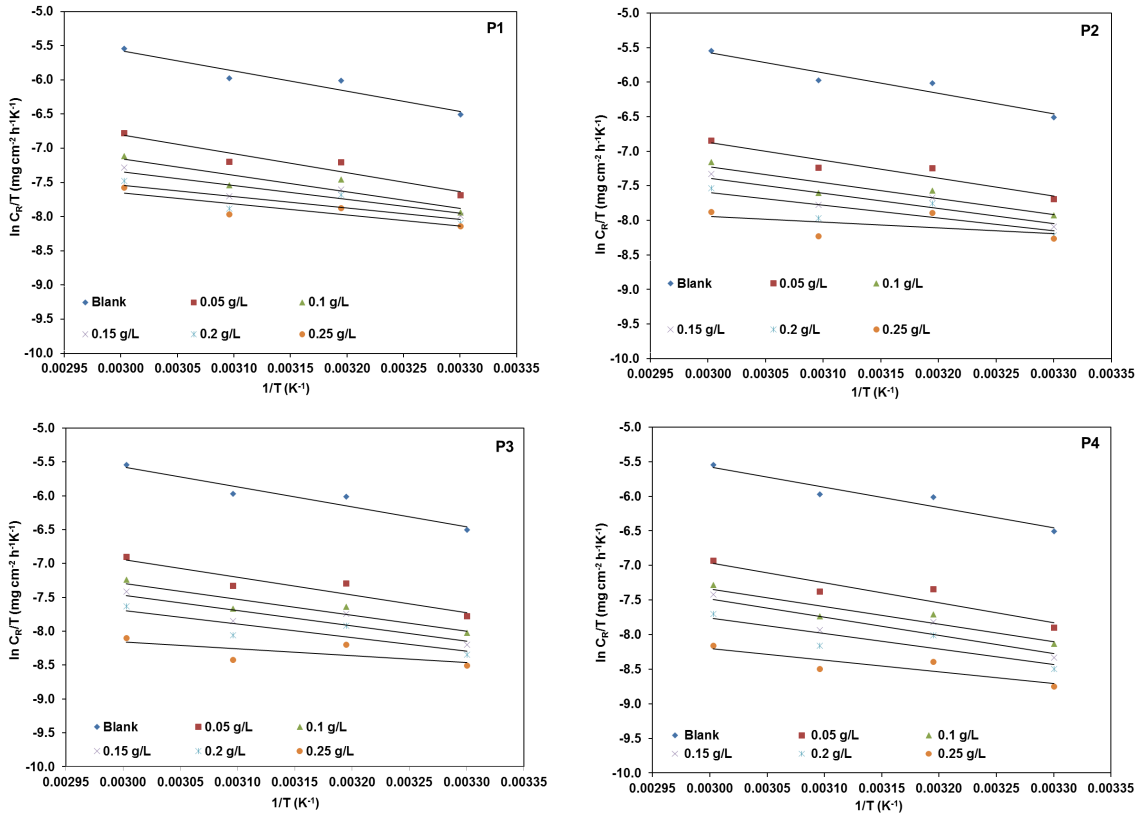

Figure 2. Alternative Arrhenius plots for mild steel in 0.5 M HCl in the absence and presence of different concentrations of (a) P1 (b) P2 (c) P3 and (d) P4.

Usually values of ΔG_{ads} up to -20 kJ/mol are consistent with the electrostatic interaction between the charged molecules and the charged metal (physisorption) while those negative values higher than -40 kJ/mol involve sharing or transfer of electrons from the inhibitor molecules to the metal surface to form a coordinate type of bond (chemisorption) [28]. Using Equation (8) and from a plot of ΔG_{ads} *vs.* T (Figure 4), the values of ΔS_{ads} and ΔH_{ads} were computed from slopes and intercepts, respectively, and the results are presented in Table 4. The values of ΔS_{ads} and ΔH_{ads} give information about the mechanism of corrosion. The negative value of ΔH_{ads} indicates that adsorption process is exothermic. An exothermic adsorption process may be chemisorption or physisorption or mixture of both [29] whereas endothermic process is attributed to chemisorption [30]. In exothermic adsorption process, physisorption can be distinguished from the chemisorption on the basis of ΔH_{ads} values. For physisorption process the magnitude of ΔH_{ads} is around -40 kJ/mol or less negative while its value -100 kJ/mol or more negative for chemisorptions [31].

In the present work, the calculated ΔG_{ads} values (Table 4) from -21.06 to -22.24, -20.70 to -21.95, -20.38 to -21.95 and -20.53 to 22.09 kJ/mol for P1, P2, P3, and P4, respectively, which indicated that the adsorption mechanism of the synthesized pyrimidine derivatives on mild steel in 0.5 M HCl solution is neither physisorption nor chemisorptions but it is a mixed type. This involves both physisorption and chemisorption (Comprehensive adsorption). The values of ΔH_{ads} again conformed that these pyrimidine derivatives adsorb on the mild steel surface probably through mixed type of adsorption.

Table 5. Impedance parameters for the corrosion of mild steel in 0.5 M HCl in presence of different concentration of the P1, P2, P3 and P4 inhibitors

Inhibitor	C (g/L)	R_{ct} (Ω.cm²)	C_{dl} (µF/cm²)	η (%)
Blank	0.00	170.4	162	-
P1	0.05	524.9	410	67.54
	0.10	655.4	203	74.00
	0.15	711.8	216	76.06
	0.20	823.1	288	79.30
	0.25	870.7	272	80.43
P2	0.05	541.2	440	68.51
	0.10	704.7	120	75.82
	0.15	835.6	297	79.61
	0.20	870.7	272	80.43
	0.25	949.0	338	82.04
P3	0.05	583.7	391	70.81
	0.10	794.9	321	78.56
	0.15	920.8	224	81.49
	0.20	1090.0	336	84.36
	0.25	1140.0	329	85.05
P4	0.05	690.7	358	75.33
	0.10	823.4	330	79.30
	0.15	959.3	134	82.24
	0.20	1079.0	240	84.21
	0.25	1231.0	232	86.16

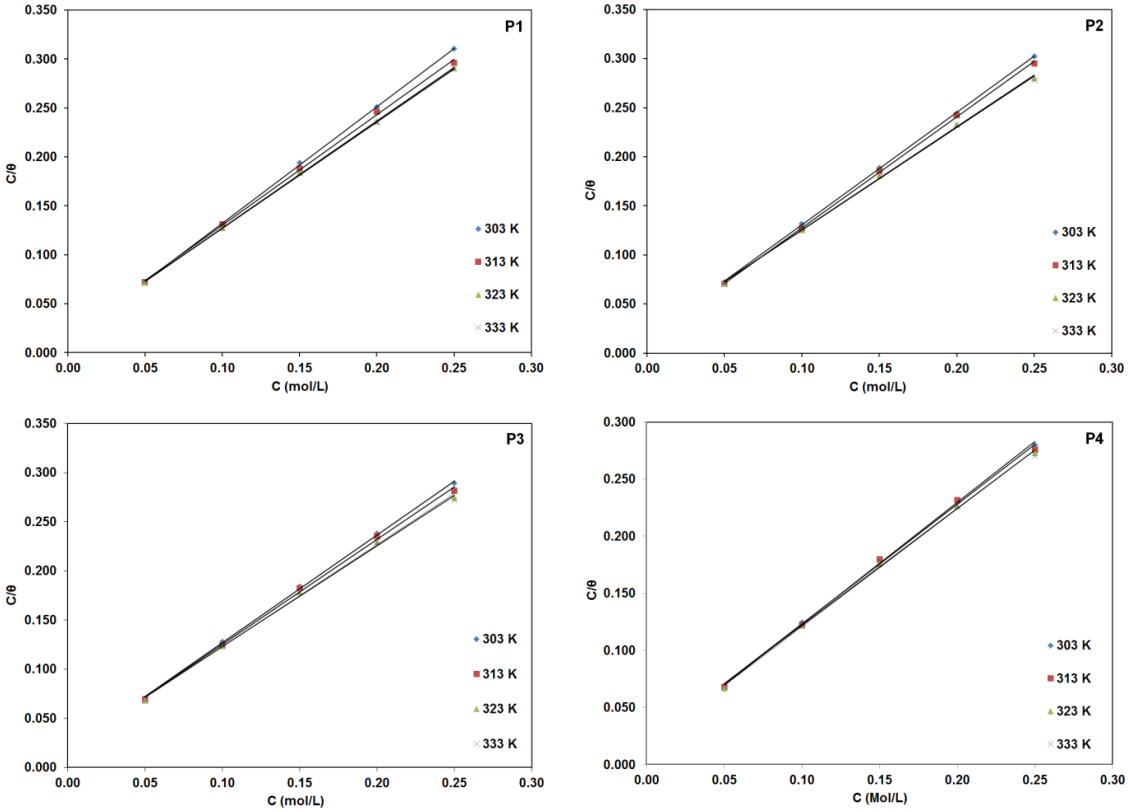

Figure 3. Langmuir isotherm for the adsorption of (a) P1 (b) P2 (c) P3 and (d) P4 on mild steel in 0.5 M HCl at different temperatures.

The value of ΔS_{ads} is negative for all the inhibitors implies that the activated complex in the rate determining step represents an association rather than a dissociation step, meaning that a decrease in disordering takes place on going from reactants to the activated complex [32].

3.2. Electrochemical impedance spectroscopy

Electrochemical impedance spectroscopy (EIS) is a powerful tool in the investigation of corrosion and adsorption phenomena. The Nyquist plots for mild steel in 0.5 M HCl in the absence and presence of P1, P2, P3 and P4 are shown in Figure 5a-5d. Nyquist impedance plots were analyzed by fitting the experimental data to a simple circuit model (Figure 6) that includes the solution resistance (R_s), charge transfer resistance (R_{ct}) and double layer capacitance (C_{dl}). The values are presented in Table 5. The η% was calculated using the charge transfer resistance as follows:

$$\eta\% = \frac{{}^{1}/_{(R_{ct})_a} - {}^{1}/_{(R_{ct})_p}}{{}^{1}/_{(R_{ct})_a}} \times 100 \quad (9)$$

where, $(R_{ct})_a$ and $(R_{ct})_p$ are charge transfer resistances in the absence and presence of inhibitor, respectively.

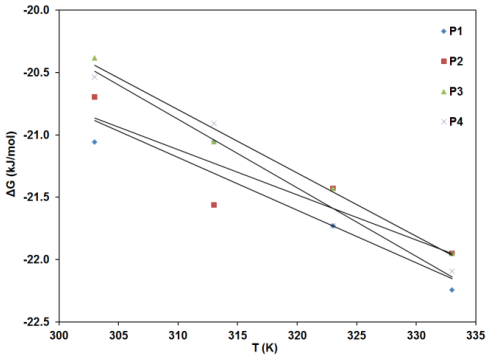

Figure 4. Plot of ΔG_{ads} *vs.* absolute temperature of P1, P2, P3 and P4.

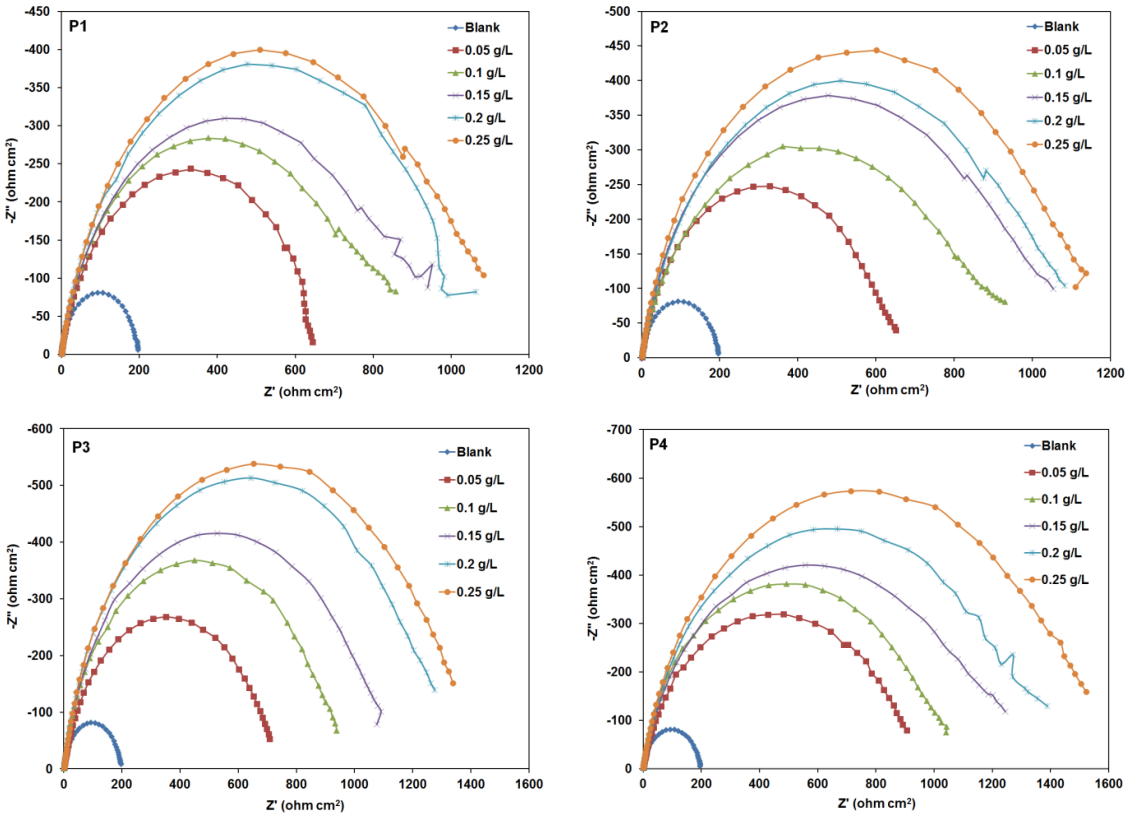

Figure 5. Nyquist plots in the absence and presence of different concentrations (a) P1 (b) P2 (c) P3 and P4 in 0.5 M HCl.

From the Nyquist plots (Figure 5a-5d), it is observed that the diameters of the capacitive loop increases with increasing concentrations of the inhibitors which specify the increasing coverage of metal surface. Further, it is clear from Table 5 that, by increasing the concentrations of inhibitors, the R_{ct} values increases. This is because, the addition of inhibitor increases the adsorption over the metal surface and results in the formation of a protective layer which may decrease the electron transfer between the metal surface and the corrosive medium [33]. The decrease in C_{dl} values with the increase in concentration of the inhibitor can be attributed to a decrease in local dielectric constant and/or an increase in the thickness of the electrical double layer which leads to an increase in the inhibition efficiency. Therefore, it is suggested that the inhibitors act by adsorption at the mild steel surface or solution interface and the change in C_{dl} values is caused by the displacement of water molecules by the adsorption of organic molecules on the metal surface, thus decreasing the extent of the metal dissolution [34].

3.3. Potentiodynamic polarization

The potentiodynamic polarization curves obtained from the corrosion behaviour of mild steel in 0.5 M HCl in the absence and presence of P1, P2, P3 and P4 inhibitors are shown in Figure 7a-7d.

The electrochemical parameters such as corrosion potential (E_{corr}), corrosion current density (I_{corr}) and Tafel slopes (i.e. cathodic (b_c) and anodic (b_a) obtained from the polarization measurements are listed in Table 6. The η% was calculated using the equation (10).

Table 6. Potentiodynamic polarization parameters for the corrosion of mild steel in 0.5 M HCl in absence and presence of different concentrations of synthesized P1, P2, P3 and P4 inhibitors at 303 K

Inhibitor	C (g/L)	E_{corr} (mV)	i_{corr} (mA/cm²)	b_a (mV dec⁻¹)	b_c (mV dec⁻¹)	η (%)
Blank	0.00	-496	0.2730	13.155	9.909	-
P1	0.05	-480	0.0883	14.002	7.806	67.60
	0.10	-468	0.0687	16.270	5.740	74.82
	0.15	-450	0.0640	16.869	5.904	76.53
	0.20	-458	0.0555	16.448	5.572	79.67
	0.25	-458	0.0525	16.657	4.890	80.74
P2	0.05	-485	0.0871	13.635	8.384	68.05
	0.10	-488	0.0676	15.231	7.855	75.22
	0.15	-482	0.0558	15.794	7.794	79.56
	0.20	-.458	0.0525	16.657	4.890	80.74
	0.25	-456	0.0513	17.283	5.648	81.20
P3	0.05	-476	0.0796	13.723	6.869	70.83
	0.10	-454	0.0580	17.052	4.332	78.74
	0.15	-444	0.0494	16.451	4.015	81.89
	0.20	-447	0.0432	16.769	4.667	84.15
	0.25	-455	0.0395	14.971	5.933	85.51
P4	0.05	-432	0.0665	20.131	2.852	75.60
	0.10	-435	0.0556	19.000	3.369	79.60
	0.15	-446	0.0464	17.408	4.239	82.98
	0.20	-441	0.0357	16.103	4.381	86.90
	0.25	-465	0.0326	15.995	6.822	88.03

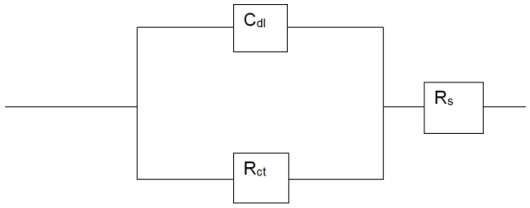

Figure 6. Electrochemical equivalent circuit used to fit the impedance.

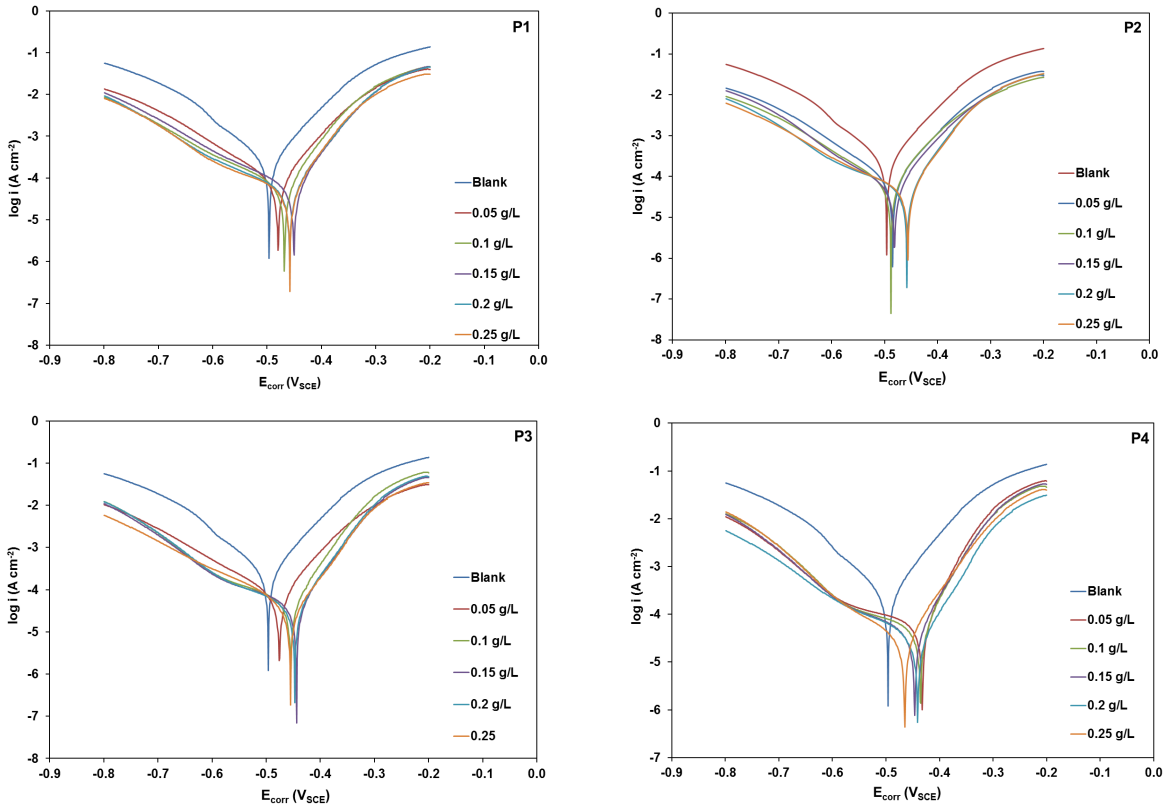

Figure 7. Polarization curves for mild steel in 0.5 M HCl containing different concentration of (a) P1 (b) P2 (c) P3 and P4.

$$\eta\% = \frac{(I_{corr})_a - (I_{corr})_p}{(I_{corr})_a} \times 100 \quad (10)$$

where $(I_{corr})_a$ and $(I_{corr})_p$ are the corrosion current density (mA cm^{-2}) in the absence and presence of the inhibitor, respectively. From the potentiodynamic polarization curves, I_{corr} value decreases considerably in the presence of P1, P2, P3, and P4 with increasing inhibitor concentration. However no definite trend was observed in the shift of E_{corr} values, in presence of various concentrations of these inhibitors. The addition of pyrimidine derivatives modifies slightly the cathodic slop. In anodic domain, the presence of P1, P2, P3 and P4 in 0.5 M HCl results in a reduction of anodic current density. These results indicated that all the four pyrimidine derivatives these inhibitors exhibit cathodic and anodic inhibitor effects. Therefore, P1, P2, P3 and P4 inhibitors can be classified as of mixed type of inhibitor. This phenomenon implies that the inhibitor could suppress anodic reaction of the metal dissolution as well as cathodic hydrogen evolution [35]. Ferreira and others [36-37] reported that, if the deviation in the E_{corr} is greater than 85 mV in inhibited system with respect to uninhibited, the inhibitor could be recognized as cathodic or anodic type whereas the deviation in E_{corr} less than 85 mV, it could be recognized as mixed type of inhibitor.

In the present investigation, the maximum deviation range is less than 85 mV for all the four inhibitors, which again conforms that P1, P2, P3 and P4 act as mixed type of inhibitors, however, the anodic effect is much more pronounced. Among the synthesized pyrimidine derivatives, P4 shows highest inhibition efficiency. The higher inhibition efficiency of P3 and P4 compare to P1 and P2 is probably due to presence of hydrazide group (-NH-NH_2) and highest inhibition efficiency of P4 among all the four is due to presence of sulphur atom in the molecule. The polarisation studies also confirms the inhibiting character of P1, P2, P3 and P4 obtained with weight loss measurements. The variation of inhibition efficiency with inhibitor concentration is represented in Figure 8. However, η% values, determined using polarisation curves were smaller than those determined by weight loss measurements. This difference is probably caused by the shorter immersion time in the case of polarisation measurements. The order of inhibition efficiency was P4 > P3 > P2 > P1.

3.4. Morphological Investigation

The SEM micrographs obtained for the mild steel surface in the absence and presence of optimum concentration (0.25 g\L) of the inhibitors in 0.5 M HCl at 6 h immersion time and 30 °C are shown in Figure 9a-9d. The image of the polished mild steel is shown in Figure 9a. The mild steel surface in the absence of inhibitors exhibited a highly corroded surface with pits and cracks (Figure 9b). This is due to the attack of mild steel surface with aggressive acid medium. However, in the presence of P1 (Figure 9c), P2 (Figure 9d), P3 (Figure 9e) and P4 (Figure 9f), the mild steel surface could be observed with a thin layer of the inhibitor molecules, giving protection against corrosion. The inhibited mild steel surface was smoother than the uninhibited surface indicating the presence of a protective layer of adsorbed inhibitors. The surface film has higher stability and low permeability in aggressive solution than uninhibited mild steel surface. Hence, they show enhanced surface properties, which seemed to provide corrosion protection to the mild steel beneath them by restricting the mass transfer of reactants and products between the bulk solution and the mild steel surface.

3.5. Evaluation of inhibitor efficiency

Comparison of η(%) (Inhibition efficiency) of the compounds by all the techniques shows the following order: P4 > P3 > P2 > P1.

The two sets of compounds (P1, P3 and P2, P4) have identical general structures, except the substituents at position 2 and 5 (Table 1). The higher η% of P2 compared to P1 and P4 compared to P3 may be attributed to the presence of C=S group, which enhances the electron density on the molecule, and act as the active sites for adsorption. The variation in η% is due to different functional groups attached to the pyrimidine ring. The pyrimidine derivative (P4) with hydrazide and C=S group shows 92 % inhibition efficiency. It has been considered that, in thio compounds (P2 and P4), the active centre is the S atom even if nitrogen atoms are present. Adsorption through sulphur could be predicted on the basis of 'Hard and Soft Acid Base' principle. The metal surface having Fe^0 is a soft acid and S compounds are soft bases. An electrostatic attraction leading to a type of bonding occurs between Fe^0 and S compound and is more favourable than the bonding between soft acid Fe^0 and hard bases such as O and N centres.

According to Hoar and Holliday [38], the adsorption of an inhibitor on the metal surface will induce a partial negative charge at the point of attraction. There are two main ways by which the intensity of negative charge on the metal atom can be reduced: (i) back donation to sulphur atom and (ii) redistribution of charge at some cathodic sites. Donnelly *et al.* [39] attributed that the higher inhibition efficiency of S compounds is due to the presence of d-orbitals which interacts with some of the d-orbital of metal atoms. Overlapping occurs between the orbitals of sulphur atom and the metal, forming a partial d_π -d_π bond which decreases the residual positive charge on S and negative charge on Fe and strengthening the original electrostatic bond. In P2 and P4, the presence of C=S group acts as an additional anchoring site for adsorption leading to stronger bond with metal surface and greater inhibition. These facts are also supported by the reports of Ozcan *et al.* [40] based on quantum chemical calculations. According to them, the highest value of the HOMO density is found in the vicinity of the sulphur atom which clearly indicating that the nucleophilic centre is S atom. Thus the bond with metal and S will be easily formed rather than with N or C atoms.

4. Conclusion

1. All the studied pyrimidine derivatives show excellent inhibition property for the corrosion of mild steel in 0.5 M HCl solutions, and the inhibition efficiency increases with increasing concentration of the inhibitors and temperature of the medium.
2. The inhibition ability of these compounds follow the order P4 > P3 > P2 > P1, and the inhibition efficiencies determined by polarization, EIS and weight loss methods are in good agreement with each other.
3. The adsorption of all the studied molecules obeys the Langmuir isotherm model. The negative values of free energy of adsorption indicated that the adsorption of the pyrimidine derivatives is spontaneous process.
4. The calculated ΔG_{ads} and ΔH_{ads} values indicated that the adsorption mechanism of the synthesized pyrimidine derivatives on mild steel in 0.5 M HCl solution is physisorption.
5. SEM analysis shows that the formed surface film has higher stability and low permeability in aggressive solution than uninhibited mild steel surface. Hence, they show enhanced surface properties.
6. The highest inhibition efficiency of P4 is due to the presence of C=S group, which enhances the electron density on the molecule, and act as the active sites for adsorption.

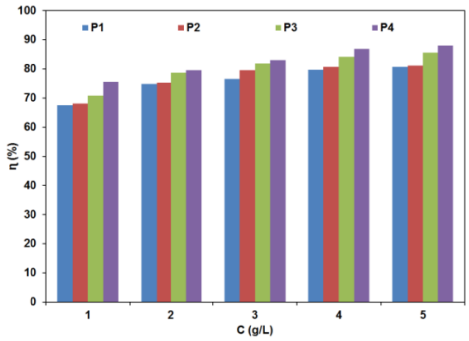

Figure 8. Variation of inhibition efficiency with inhibitor concentration in polarization studies.

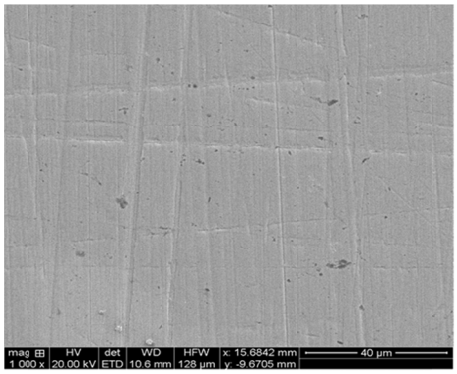

(a)

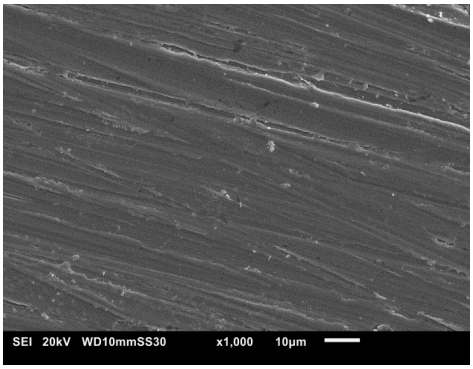

(b)

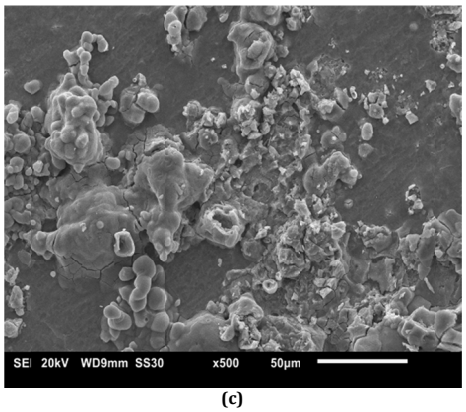

(c)

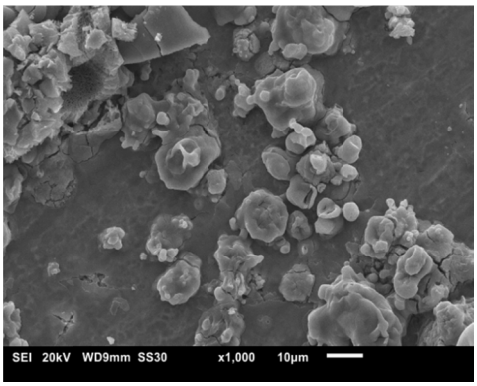

(d)

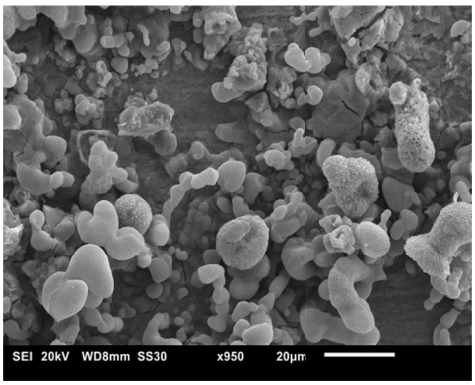

(e)

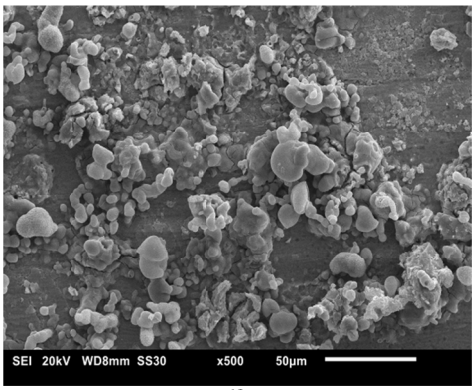

(f)

Figure 9. SEM images of mild steel in 0. 5 M HCl after 6 h immersion at 30 °C (a) before immersion (polished) (b) without inhibitor (c) with 0.25 g/L of P1, (d) with 0.25 g/L of P2 (e) with 0.25 g/L of P3 and (f) with 0.25 g/L of P4.

Reference

[1]. Moretti, G.; Guidi, F.; Grion, G. *Corros. Sci.* **2004**, *46,* 387-403.
[2]. Dahmani, M.; Et-Touhami, A.; Al-Deyab, S. S.; Hammouti B.; Bouyanzer, A. *Int. J. Electrochem. Sci.* **2010**, *5,* 1060-1069.
[3]. Collins, W. D.; Weyers, R. E.; Al-Qadi, I. L. *Corrossion* **1993**, *49*, 74-78.
[4]. Obot, I. B.; Obi-Egbedi, N. O.; Umoren, S. A. *Corros. Sci.* **2009**, *51,* 276-282.
[5]. Obot, I. B.; Obi-Egbedi, N. O. *Surf. Rev. Lett.* **2008**, *15*, 903-910.
[6]. Ashassi-Sorkhabi, H.; Shaabani, B.; Seifzadeh, D. *Electrochim. Acta* **2005,** *50,* 3446-3452.
[7]. Hammouti, B.; Zarrouk, A.; Al-Deyab, S. S.; Warad, I. *Oriental J. Chem.* **2011**, *27*, 23-31.
[8]. Elayyachy, M.; Hammouti, B.; El Idrissi, A.; Aouniti, A. *Port. Electrochim. Acta*. **2011**, *29*, 57-68.
[9]. Zarrouk, A.; Warad, I.; Hammouti, B.; Dafali, A.; Al-Deyab, S. S.; Benchat, N. *Int. J. Electrochem. Sci.* **2010**, *5,* 1516-1526.
[10]. Khaled, K. F.; Abdelshafi, N. S.; El-Maghraby, A.; Al-Mobarak, N. *J. Mater. Environ. Sci.* **2011**, *2*, 166-173.
[11]. Chetouani, A.; Hammouti, B.; Aouniti, A.; Benchat, N.; Benhadda, T. *Prog. Org. Coat.* **2002**, *45,* 373-378.
[12]. Wang, L. *Corros. Sci.* **2006**, *48,* 608-616.
[13]. Bentiss, F.; Gassama, F.; Barbry, D.; Gengembre, L.; Vezin, H.; Lagrenee, M.; Traisnel, M. *Appl. Surf. Sci.* **2006**, *252,* 2684-2691.
[14]. Ghazoui, A.: Saddik, R.; Guenbour, M.; Benchat, N.; Hammouti, B.; Al-Deyab, S. S. Zarrouk, A. A. *Int. J. Electrochem. Sci.* **2012**, *7*, 7080-7097.
[15]. Elewady G. Y. *Int. J. Electrochem. Sci.* **2008**, *3*, 1149-1161
[16]. Zarrok, H.; Saddik, R.; Oudda, H.; Hammouti, B.; El Midaoui, A.; Zarrouk, A.; Benchat, N.; Ebn Touhami, M. *Der Pharma Chemica* **2011**, *3,* 272-282.
[17]. Vasantasree, V.; Ranachan, T. Z. *J. Electro Chem*. **1996**, *15,* 71-75.
[18]. Ayre, J. A; Corrosion Aspects of Reactor Decontamination and Corrosion of Reactor Materials, International Atomic Agency, Wien, 1962, 199.
[19]. Akhaja, T. N.; Raval, J. P. *Eur. J. Med. Chem.* **2011**, *46,* 5573-5579.
[20]. Zhao, W. Li, X.; Liu, F. L.; Hou, B. *Corros. Sci.* **2008**, *50*, 3261-3266.
[21]. Chetouani, A.; Hammouti, B.; Aouniti, A.; Benchat, N.; Benhadda, T. *Prog. Org. Coat.* **2002**, *45*, 373-378.
[22]. Ita, B. I.; Offiong, O. E. *Mater. Chem. Phys*. **2001**, *70*, 330-335.
[23]. Ehteram, A. N. *Int. J. Electrochem. Sci.* **2007**, *2*, 996-1017.
[24]. Putilova, I. N.; Balezin, S. A.; Baranik. Metallic Corrosion Inhibitors, Pergamon Press, New York, 1960.
[25]. Popova, A.; Sokolova, E.; Raicheva, S.; Chritov, M. *Corros. Sci.* **2003**, *45*, 33-41.
[26]. Quartarone, G.; Moretti, G.; Tassan, A.; Zingales, *Werkst. Korros.* **1994**, *45*, 641-647.
[27]. Ramesh, S. V.; Adhikari, V. *Bull. Mater. Sci.* **2007**, *31*, 699-711.
[28]. Bensajjay, E.; Alehyen, S.; Achouri, M. E.; Kertit, S. *Anti-Corros. Method M*. **2003**, *50* 402-409.
[29]. Ashassi-Sorkhabi, H.; Eshaghi, M. *Mater. Chem. Phys.* **2009**, *114,* 267-271.
[30]. Bentiss, F.; Lebrini, M.; Lagrenee, M. *Corros. Sci.* **2005**, *47 (12),* 2915-2931.
[31]. Mertens, S. F.; Xhoffer, C.; Decooman, B. C.; Temmerman, E. *Corrosion* **2000**, *53 (5),* 381-388.
[32]. Behpour, M.; Ghoreishi, S. M.; Soltani, N.; Salavati-Niasari, M.; Hamadanian, M.; Gandomi, A. *Corros. Sci.* **2008**, *50*, 2172-2181.
[33]. Tang, Y.; Yang, X.; Yang, W.; Wan, R.; Chen, Y.; Yin, X. *Corros. Sci.* **2010**, *52*, 1801-1808.
[34]. Mc-Cafferty, E.; Hackerman, N. *J. Electrochem. Soc.* **1972**, *119,* 146-154.
[35]. Martinez, S.; Hucovic, M. M. *J. Appl. Electrochem.* **2003**, *33*, 1137-1142.
[36]. Ferreira, E. S.; Giancomelli, C.; Giacomelli, F. C.; Spinelli, A. *Chem. Phys. Lett.* **2004**, *83*, 129-134.
[37]. Li, W. H.; He, Q.; Zhang, S. T.; Pei, C. L.; Hou, B. R. *J. Appl. Electrochem.* **2008**, *38*, 289-295.
[38]. Hoar, T. P.; Holliday, R. D. *J. Appl. Chem.* **1953**, *3*, 502-513.
[39]. Donnelly, B.; Downie, T. C.; Grzeskowiak, R. *Corros. Sci.* **1974**, *14*, 597-606.
[40]. Ozcan, M.; Dehri, I. *Prog. Org. Coat.* **2004**, *51*, 181-187.